

# QUASI-RESONANT MULTI-OUTPUT DC/DC CONVERTER WITH PUSH-PULL TOPOLOGY

L. Rossetto\* G. Spiazzi\*\* P. Tenti\*\*

\*Department of Electrical Engineering  
\*\*Department of Electronics and Informatics  
University of Padova  
Via Gradenigo 6/a - 35131 Padova - ITALY  
Tel:+39-49-828.7500 Fax:+39-49-828.7599

F. Brasola L. Fontanella G. Patechi

NECSY - Network Control Systems - SpA  
Via Lisbona 28 -35020 Padova - ITALY  
Tel:+39-49-8291511 Fax:+39-49-778100

**Abstract :** A multi-output quasi-resonant converter suitable for applications up to several hundreds of Watts is presented. It employs a zero-current-switched full-wave push-pull structure, which allows good cross-regulation of the output voltages, high power density and full exploitation of the transformer core.

After an analysis of operation, design criteria are given and experimental results of a three-output, 100 W industrial prototype for telecom applications are reported.

## 1. INTRODUCTION

In the effort to increase the power density of power supplies, the switching frequency is pushed to high values which, in PWM converter realizations, normally lead to considerable power loss and high electromagnetic pollution. Even if the increased switching frequency does not cause unacceptable switching losses, the oscillations caused by converter parasitic elements may cause high current and voltage stresses, which are almost unpredictable, depending on circuit layout. Suitable snubber circuits must therefore be adopted, which affect power density and converter reliability.

A solution is given by quasi resonant topologies, originally introduced in [1] and deeply analysed in [2], which are now turning into wide industrial application due to their small size, limited radio-frequency disturbances and absence of switch current and voltage spikes.

Several single-output commercial converters are now available, mostly based on zero-current-switched (ZCS) half-wave (HW) topologies.

Instead, commercial multiple-output power supplies normally use hard-switched topologies [3], although solutions based on resonant switches have already been discussed in the literature [4-5].

This paper presents a multi-output ZCS full-wave (FW) converter suitable for applications up to several hundreds of Watts. Owing to full-wave structure, the switching frequency depends moderately on the load, allowing good cross-regulation of the output voltages. Moreover, as compared to

zero-voltage-switched (ZVS) full-wave topologies, the proposed solution does neither require reverse-blocking switches nor produces additional voltage stresses on the switches.

The push-pull topology is adopted in order to speed up reset of magnetic flux in the transformer core. This allows a higher duty-cycle of the switches and a greater power density of the equipment.

Based on the proposed solution, a three-output, 75 W industrial prototype for telecom applications has been developed. It works at 500 kHz and employs a standard-technology transformer.

## 2. SELECTION OF TOPOLOGY

The goal of this work is to develop an isolated multi-output zero-current-switching quasi-resonant converter for telecom applications. Taking into account the range of regulation and desired power density, buck-type topologies seem preferable over other, e.g. buck-boost structures. Moreover, the needs for multiple outputs and full exploitation of the transformer core give further constraints to the adopted solution. In the following different approaches are analysed and compared.

### A) Single or multiple resonant capacitor

In order to exploit transformer leakage inductances, secondary-side resonance is commonly adopted, in which the resonant capacitor is moved from the primary to the secondary side of the transformer [8]. An open question in resonant multi-output converters is the position of such a resonant capacitor: concentrated on the secondary side of the main output or distributed in all transformer secondaries. If resonant inductors were concentrated in the primary winding, with the secondaries perfectly coupled, the two solutions would be equivalent. Instead, not negligible secondary leakage inductances, together with the parasitic capacitances

of the rectifying diodes, give rise to uncontrollable oscillations. External resonant capacitors are therefore needed in each secondary winding to set the proper resonant frequency.

This approach differs from that followed in [5], in which only the main output has a quasi-resonant structure whereas the auxiliary one is considered as a standard PWM topology.

#### B) Forward vs. push-pull

The simplest buck-type topology performing high-frequency insulation is the forward converter. It needs only one switch with a simple transformer core. Moreover, reset of the magnetizing current can be obtained, without auxiliary windings, by taking benefit of the resonance between magnetizing inductance and output capacitance of the mosfet. However, since the magnetizing inductance cannot be reduced beyond a certain value and the mosfet output capacitance is given once the device is selected, the time required to reset the transformer core can be not negligible as compared to the resonance period. This results in an upper limitation of the duty-cycle, affecting converter power density. Moreover, if full-wave operation is chosen, during turn off interval the resonant capacitors appear in parallel to the mosfet output capacitance, thus increasing the reset time.

These problems can be overcome by a push-pull topology, in which core reset is ensured by complementary operation of the switches.

#### C) Half-wave vs. full-wave operation

As known, half-wave operation has the advantages of higher efficiency (due to less circulating energy) and simple structure (secondary rectifier diodes are the blocking devices providing half-wave operation). The main drawback arises from voltage conversion ratio sensitivity to load variations. This means that the switching frequency may change a lot in order to stabilize the output voltage in presence of variations. This is not acceptable, in multiple-output implementations, since non-regulated output voltages may vary greatly for any load variation of the main output. In this case, full-wave operation, which has a voltage conversion ratio theoretically independent of the load, is the only choice.

#### D) Proposed topology

The proposed converter structure is a push-pull zero-current-switching quasi-resonant converter in full-wave operation, as shown in Fig.1. As we can see, bridge rectifiers, although characterized by higher conduction losses, have been preferred over center-tap rectifiers, so as to reduce transformer windings size. Moreover, in order to limit the conduction loss in the free-wheeling status, a free-wheeling diode has been connected across each converter output.

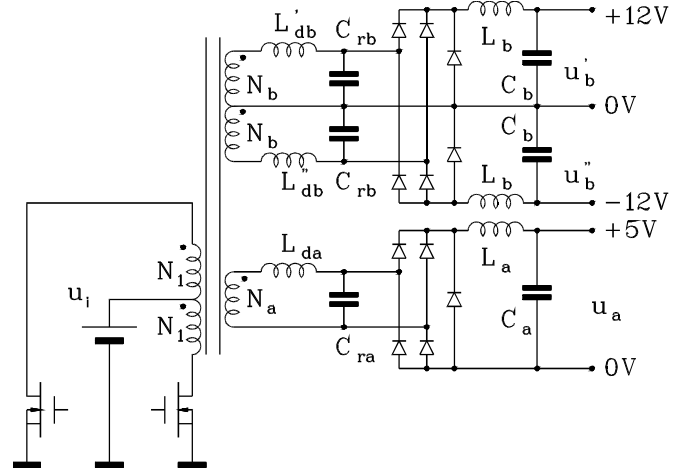


Fig. 1 - Converter schematic

#### A) Single-output configuration: ideal behavior

Prior to discuss the characteristics of a multi-output converter it is worthwhile to analyse the behavior of a normal push-pull ZCS-QRC, whose structure and basic waveforms are shown in Fig.2. As already described in [1], the switching period is divided in the four sub-intervals  $T_{ij}$  ( $i=0, \dots, 3$   $j=i+1$ ), each associated to one sub-topology shown in Fig.3. The analysis is based on the assumptions that output filter and load behave as a constant current sink, and that semiconductor switches and resonant components are ideal. We define:

$$\text{Characteristic impedance} \quad Z_r = \sqrt{\frac{L_r}{C_r}} \quad (1)$$

$$\text{Resonant angular frequency} \quad \omega_r = \frac{1}{\sqrt{L_r C_r}} \quad (2)$$

$$\text{Resonant frequency} \quad f_r = \frac{\omega_r}{2\pi} \quad (3)$$

The behavior is the following. When the switch is off ( $t < T_0$ ), the freewheeling diode is carrying the load current. During interval  $T_{01}$ , the switch is on and the resonant inductor current rises linearly until it reaches the output current value. When this happens, the freewheeling diode is turned off and the resonance takes place (interval  $T_{12}$ ). In full-wave operation, the resonant current can reverse polarity, flowing through the body diode of the mosfet, which can be turned off at zero current. During interval  $T_{23}$ , the resonant capacitor is linearly discharged by the

### 3. PRINCIPLE OF OPERATION

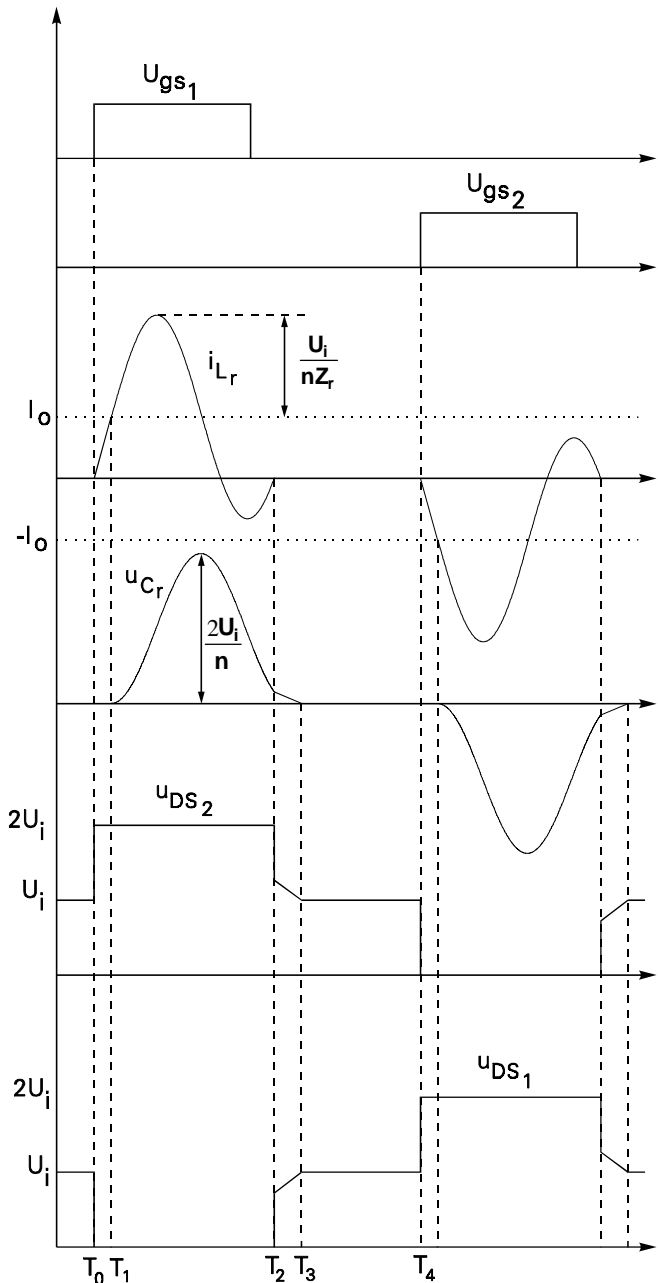
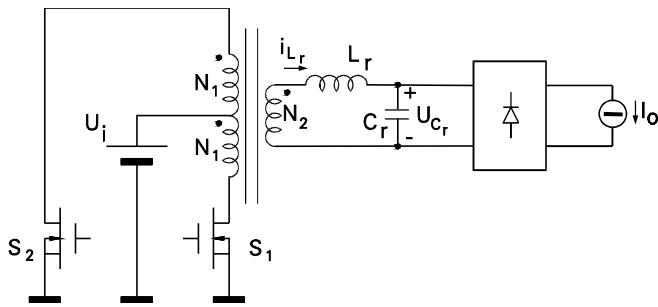


Fig.2 - Ideal push-pull QRC waveforms

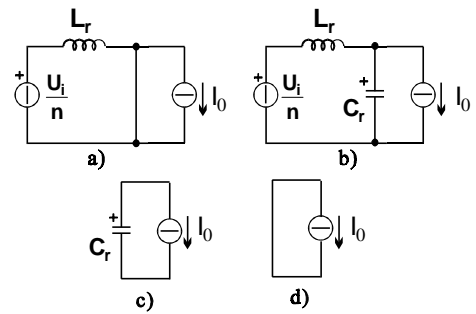


Fig.3 - Equivalent circuits of the ideal push-pull converter in four topological stages: a) inductor-charging stage  $T_{01}$ , b) resonant stage  $T_{12}$ , c) capacitor-discharging stage  $T_{23}$ , d) freewheeling stage  $T_{34}$

output current and when its voltage reaches zero, the freewheeling diode starts to conduct. This interval ( $T_{34}$ ) ends when the switch is turned on, starting a new switching cycle.

As we can see, the resonant capacitor is almost totally discharged by the resonant current, giving rise to a voltage conversion ratio virtually independent of the load current. In fact, since output voltage equals average resonant capacitor voltage, we can write:

$$M = \frac{nU_0}{U_i} \approx \frac{f_s}{f_r} \quad (4)$$

where  $f_s$  is the switching frequency seen from the load (actual switch commutation frequency is  $f_s/2$ ) and  $n$  is transformer turns ratio ( $n=N_1/N_2$ ). Thus, the ratio switching-frequency to resonant-frequency plays the rule of duty-cycle in the corresponding PWM structure.

### B) Multi-output case

In our multi-output implementation, if transformer leakage inductances are concentrated in the secondary windings, the three outputs perform independently from each other. In this case, even if all secondary circuits have the same resonance frequency, instants  $T_i$  of Fig.2 do not coincide for the various circuits, since they depend on the corresponding load currents. Thus, the switch current, which is the sum of all secondary currents (reflected to the primary side) and the magnetizing current, will not generally have the simple behavior of  $i_{Lr}$  in Fig.2: in particular, the negative peaks of the resonant currents will not be synchronized. This, together with the presence of a magnetizing current, calls for oversizing the resonant circuits, in order to achieve zero-current switching.

On the other hand, if transformer leakage inductances were concentrated in the primary windings, the precision of the auxiliary output voltages should be guaranteed only by the turns ratio, while the problem of imbalanced oscillations would disappear. It is important to note that in this case the voltage stress on the switches would be three times larger than the input voltage, while in the previous case it is only twice (as depicted in Fig.2). This happens because, during

resonance interval  $T_{12}$ , the resonant capacitor voltage is reflected to the primary side and adds to the input voltage.

### C) Transformer core reset

An important issue related to push-pull structure is magnetizing current behavior. In standard applications, current-mode control is adopted to avoid volt-second mismatch across magnetizing inductance. Here, an inherent balance mechanism of the magnetizing current is ensured by the current-dependent turn-off time of the switches. In fact, the effective length of turn-on interval is determined by the instant in which the body diode current zeroes. Therefore, if magnetizing current tends to increase the body diode stops earlier, limiting the volt-seconds applied. This clearly represents a negative feedback action against magnetizing current variations.

## 4. POWER STAGE DESIGN

Since each output circuit can be considered independent of the others, only the design procedure for the main output is reported.

The converter specifications are usually expressed in terms of:

- minimum and maximum input voltage:  $U_{i,\min}$ ,  $U_{i,\max}$
- rated output voltage  $U_0$
- rated output current  $I_0$
- maximum switching frequency  $f_{s,\max}$

### A) Choice of transformer turns ratio

From the converter efficiency point of view, it is desirable to have a high turns ratio which reduces primary current amplitude. This is obtained by operating the converter at the maximum duty-cycle (theoretically unity). In practice, however, because of the required dead-time, a maximum duty-cycle  $k_t$  equal to 0.8 is chosen. Thus we can write:

$$n = \frac{U_{i,\min} - U_{DS,on}}{U_0 + \Delta U_{loss}} \cdot k_t \quad (5)$$

where  $U_{DS,on}$  is voltage drop on the conducting mosfet and  $\Delta U_{loss}$  is DC voltage drop on secondary diodes and output inductor.

As far as the other turns ratio is concerned, it is chosen according to the corresponding voltage gain.

### B) Choice of resonant elements

The characteristic impedance of the resonant circuit must be chosen in order to guarantee zero-current switching in the worst condition, i.e. with minimum input voltage and maximum load current. The condition for ZCS is:

$$Z_r \leq \frac{U_{i,\min} - U_{DS,on}}{n I_0} \quad (6)$$

Note that the value of  $Z_r$  heavily affects the current stress in the switches, so that the maximum value permitted by (6) is usually chosen. However, in the multi-output converter the actual switch current is given by the sum of transformer magnetizing current and resonant inductor currents reflected to the primary side. Thus, taking into account the lack of synchronisation of the resonant currents, a lower value of  $Z_r$  must generally be adopted to ensure zero-current switching.

Given the maximum switching frequency, from (4) and (5) the resonant frequency is calculated by:

$$\frac{f_{s,\max}}{f_r} \approx k_t \Rightarrow f_r \approx \frac{f_{s,\max}}{k_t} \quad (7)$$

Resonant elements are therefore given by:

$$L_r = \frac{Z_r}{\omega_r}, \quad C_r = \frac{1}{Z_r \omega_r} \quad (8)$$

### C) Switching frequency range

When input voltage changes, switching frequency must change accordingly, in order to maintain the desired output voltage. From (4) we can easily derive:

$$\frac{f_{s,\max}}{f_{s,\min}} \approx \frac{U_{i,\max}}{U_{i,\min}} \quad (9)$$

### D) Choice of output filter elements

Selection of output filter elements proceeds as for standard PWM converters. In particular, the output inductor can be designed to achieve continuous-current-mode operation (CCM) for any load conditions. Alternatively, discontinuous-current-mode (DCM) can be tolerated at light load to reduce the inductance value and, at the same time, its parasitic resistance. In this latter case, a saturable inductor can be put in series to the main one in order to reduce current ripple at light load.

## 5. CONTROL CIRCUIT DESIGN

As for any ZCS-QRC, the switches operate with constant on time and control changes the switching frequency in order to face input voltage and load variations.

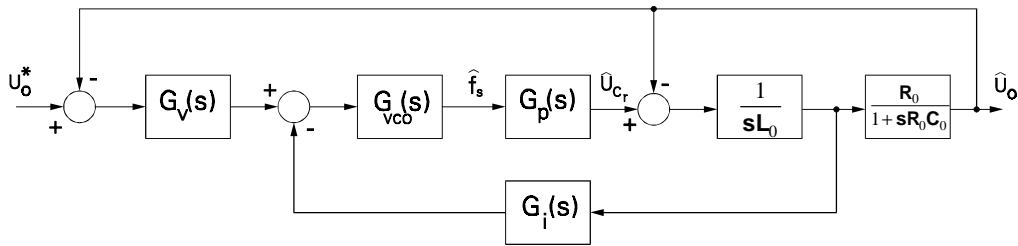


Fig.4 - Control block scheme

Given the small-signal behavior of the power stage, the error amplifier is designed so as to provide the required dynamic performances. It has already been shown that QRCs have small-signal characteristics similar to their PWM counterparts [7]. Moreover, in order to increase the crossover frequency, while ensuring stability in all operating conditions, multi-loop controls (e.g. including a current loop) can be profitably applied [8].

In our case, an average current control was adopted, whose block scheme is shown in Fig.4 where  $L_0$ ,  $C_0$  and  $R_0$  are output filter components and load resistance, respectively. Transfer function  $G_v(s)$  is a PI regulator, while  $G_i(s)$  is a simple constant gain. It is worthy to note that, in the particular implementation used, the voltage controlled oscillator (VCO) has a transfer function which depends on the square of the frequency. This is preferable because it gives less sensitivity to the output current ripple at light load, when converter enters discontinuous operation mode and switching frequency is minimum.

## 6. CONVERTER IMPLEMENTATION

From the practical point of view, design is mainly determined by the transformer technology, which heavily influences any aspect of the circuit behavior, including commutation frequency and efficiency.

In our case, no special (e.g., "flat") transformer cores have been used, since the associated costs can be unacceptable for small-production-volume applications (however, ferrites suitable for high-frequency applications, namely Philips 3F3, have been employed). The switching frequency is therefore smaller than that theoretically allowed by resonant-switch technology. Nevertheless, results are interesting, because they demonstrate the feasibility of industrial applications of quasi-resonant topologies in conjunction with standard technologies of transformers and other reactive elements.

The main ratings of the developed converter are:

- Dc supply  $U_i$ : ..... 38-72 V
- Controlled (main) output  $U_a$ : ..... 5 V - 10 A
- Secondary (dual) outputs  $\pm U_b$ : .....  $\pm 12$  V - 1 A

- Maximum switching frequency  $f_{s,max}$ : ..... 500 KHz

while the circuit parameters are:

- Number of turns:  $N_1 = 6$ ,  $N_a = 3$ ,  $N_b = 7$
- Transformer leakage inductances (secondary side):  
 $L_{da} = 160$  nH,  $L'_{db} = 512$  nH,  $L''_{db} = 658$  nH
- Transformer parasitic capacitances (primary side): 800 pF
- Magnetizing inductance (primary side): 126  $\mu$ H
- Resonant capacitors:  $C_{ra} = 50$  nF,  $C_{rb} = 10$  nF
- Output filters:  
 $L_a = 45$   $\mu$ H;  $L_b = 200$   $\mu$ H;  
 $C_a = C_b = 1000$   $\mu$ F

Note the very small values of the leakage inductances. In fact, transformer design was optimized with this respect, so as to increase the switching frequency.

Design parameters were verified by simulation with SABER, taking into account transformer parasitics and component nonidealities.

## 7. EXPERIMENTAL RESULTS

Figs.5-7 show the main converter waveforms, measured in the following conditions:  $U_i=50$ V,  $I_{0a}=3.5$ A and bleeder resistances on the auxiliary outputs.

Fig.5 shows the voltage across the switches. As we can

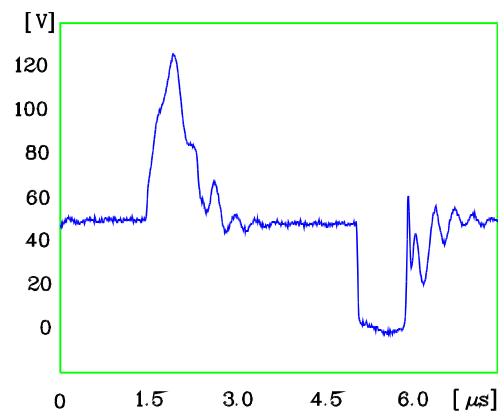


Fig.5 - Switch voltage

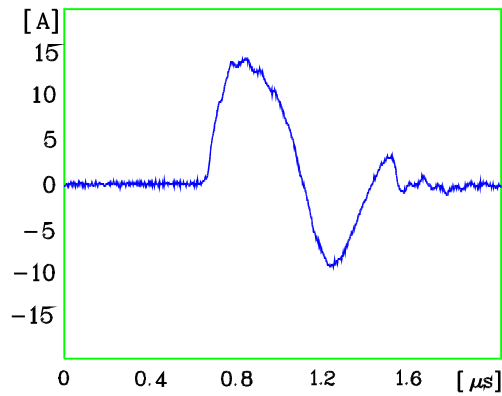


Fig.6 - Switch current

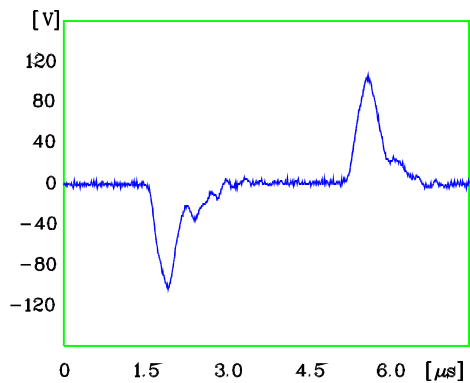


Fig.7 - Resonant capacitor voltage

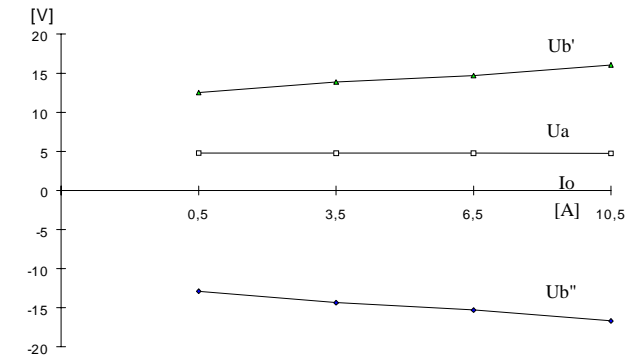


Fig.8 - Cross-regulation characteristic

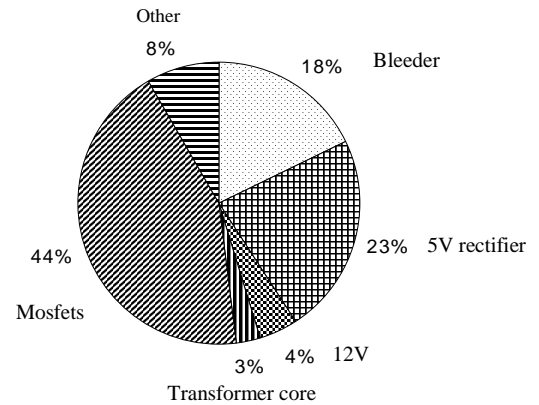


Fig.9 - Losses distribution

observe, during conduction of the other mosfet the voltage behavior differs from that (ideal) of Fig.2, showing that the leakage inductances are split between primary and secondary windings. Accordingly we can expect a voltage stress is in the range  $2U_i \div 3U_i$ .

The switch current, reported in Fig.6, shows a tail due to recovery of the mosfet body diode.

Fig.7 shows the voltage on resonant capacitor  $C_{rb}$ .

Fig.8 illustrates the cross-regulation characteristic of the converter (for  $U_c = 48$  V). The main output current varies from zero to the rated value, while other outputs feed the rated load (worst condition). The non-controlled output voltages change about 13%. It is interesting to note that coupling the output inductors makes worse cross-regulation, since the voltages applied to the output inductors are not well matched.

Fig.9 shows distribution of the power losses. The main loss factors are the Mosfets, followed by the output rectifiers. Other losses are less important. The measured efficiency at  $U_i=50$ V with rated power was 70%, including control losses.

Lastly, Fig.10 gives the spectrum of conducted noises in the supply bus. This behavior complies with MIL standards, although the RF filter is relatively simple and cheap. The measurement was done with LISN EMCO standard network.

Fig.10 - Spectrum of conducted noise

## 8. CONCLUSIONS

A multi-output quasi-resonant dc/dc converter has been presented, which is characterized by good cross-regulation and efficiency, and reduced injection of RF harmonics in the supply bus. It uses a push-pull switching stage with standard-technology transformer, and allows high power density and full exploitation of the magnetic flux swing.

Experimental results of an industrial prototype demonstrate actual converter performances.

### References:

- [1] - K.H.Liu, R.Oruganti, F.C.Lee, "Resonant switches - Topologies and characteristics," Proc. of IEEE PESC Conf., 1985, pp.106-116.
- [2] - F.C.Lee, Editor, "High frequency resonant, quasi-resonant and multi-resonant converters," VPI-VPEC Press, 1989.
- [3] - F.Kurokawa, H.Matsuo, "A new multiple-output hybrid power supply," IEEE Trans. on Power electronics, vol.PE-3, n.4, 1988, pp.412-419.
- [4] - W.A.Tabisz, F.C.Lee, "Design of high-density on-board single- and multiple-output multi-resonant converters," Proceedings of HFPC Conf., 1990, pp.61-73.
- [5] - P.Croll, G.Grellet, "Multiple output DC/DC zero-current switch quasi-resonant converter," INTELEC Conf. Proc., 1993, pp.215-220.
- [6] - K.H.Liu, F.C.Lee, "Secondary-side resonance for high-frequency power conversion," IEEE APEC Conf. Proc., 1986, pp.83-89.
- [7] - V.Volperian, k.H.Liu, R.Tymerski, F.C.Lee, "Generalized resonant switches, part 2: analysis and circuit models," VPEC Seminar Proc., 1986, pp.124-131.
- [8] - R.B.Ridley, F.C.Lee, V.Volperian "Multi-loop control for quasi-resonant converters," HFPC Conf. Proc., 1987.